Available online at www.sciencedirect.com

ScienceDirect

Mendeleev Commun., 2020, **30**, 198–201

Mendeleev Communications

Synergistic effect in Co–zeolite catalyzed transformations of hydrocarbons under Fischer–Tropsch conditions

Lilia V. Sineva,* Ekaterina O. Gorokhova, Ekaterina V. Kulchakovskaya, Ekaterina Yu. Asalieva, Ekaterina A. Pushina, Alexey N. Kirichenko and Vladimir Z. Mordkovich

Technological Institute for Superhard and Novel Carbon Materials, 108840 Troitsk, Moscow, Russian Federation. Fax: +7 499 400 6260; e-mail: sinevalv@tisnum.ru

DOI: 10.1016/j.mencom.2020.03.023

HBeta and HZSM-5 zeolites as well as zeolite-based Co catalysts are active in various transformation reactions of liquid hydrocarbons, *e.g.*, the Fischer–Tropsch synthesis, in the temperature range of 170–260 °C. The conversion and distribution of liquid and gaseous products in case of hydrocarbon mixture transformation does not follow the pattern set by individual hydrocarbons. The results cannot be interpreted by simple superposition of individual hydrocarbon reactions thus revealing a synergistic effect.

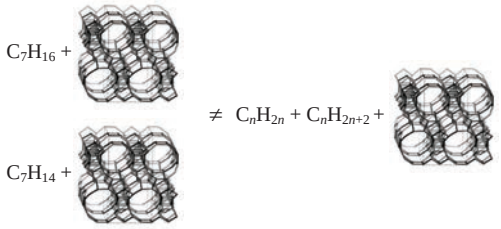

Keywords: hydrocarbons, zeolites, synergistic effect, Fischer–Tropsch synthesis, multifunctional catalysis.

The Fischer–Tropsch synthesis (FTS) is a key stage of a family of alternative fuel technologies.[1] Cobalt is used as an active metal in most FTS catalysts because it provides liquid hydrocarbons with minimum undesirable oxygenates and aromatics. The technologies implemented in the industry on the basis of cobalt catalysts are focused on obtaining high-molecular hydrocarbons for their subsequent hydrocracking. On the other hand, zeolites are widely used in petrochemical cracking processes.[2] It looks quite attractive to combine cobalt and zeolites as active components in a single catalytic system.[3–6]

The previous research demonstrated that the development of new multifunctional FTS catalysts based on a combination of several types of active centers in one catalyst meets a challenge for rationalization of secondary transformations of hydrocarbons occurring at the active centers of zeolites and Co.[3–8] Importantly, composition of the final products of the FTS performed in the presence of Co–zeolite systems depended on the distance between the active centers of zeolite and cobalt.[7]

The reports on the zeolites for hydrocarbon processing[9,10] describe the catalysis at temperatures significantly higher than those characteristic for FTS in the presence of Co catalysts, while the data on zeolite catalytic activity in the temperature range of 170–260 °C are scarce. There is no doubt, however, that the composition of liquid hydrocarbons obtained in the presence of mixed Co–zeolite catalysts should depend largely on the properties of zeolite.[11]

The purpose of this work was to study the influence of zeolite structural type on hydrocarbon transformations in the presence of zeolites and hybrid Co–zeolite catalysts under Fischer–Tropsch conditions, namely within 170–260 °C temperature range.

HZSM-5 and HBeta zeolites (Zeolyst) with Si/Al ratios of 1 : 19 and 1 : 12.5, respectively, were used as representatives of distinctively different types. Zeolite HZSM-5 is a subject of major publications on petroleum cracking, while HBeta is proven to be promising in multifunctional catalysis.[7] The zeolites were used in catalytic experiments in the pristine form, while the Co–zeolite catalysts were prepared by impregnation of zeolite-containing supports[†] to reach 20 wt% Co.

Conversion of hept-1-ene into gaseous products manifested no significant temperature dependence and never exceeded 0.5% (Figure 1). The gaseous products of this transformation were dominated by C_4 hydrocarbons with butane:butene ratio growing with temperature from 0.2–0.4 up to 0.8–3.5 (Figure 2). It is of interest that content of propene grew with temperature from almost zero up to 30 mol%, while neither methane nor ethane were detected [Figure S1(*b*), Online Supplementary Materials]. An unexpected appearance of CO_2 and CO was observed at all the temperatures with their yields rising with temperature growth up to 9 and

[†] The supports were prepared by extrusion and consequent annealing of a paste comprising zeolite (20 wt%), boehmite (50 wt%) and flaky graphite (20 wt%, heat-conductive component). The paste also contained liquid phase with peptizer and plastisizer. A special reference catalyst sample (referred to as Ref) was prepared with the use of a zeolite-free paste. The pellet size was 1.5 mm in diameter and 1.5–2 mm in length. Zeolites and mixed catalysts were activated in a hydrogen flow at 400 °C and 0.1 MPa for 1 h, which is typical for FTS catalysts of this type (see ref. 7). The catalytic experiments were performed in a vertical stainless flow reactor with inner diameter of 10 mm at 0.1 MPa. Liquid hydrocarbon feedstock was fed into helium flow at 0.02 ml min^{-1} rate by a syringe pump. The temperature was raised stepwise, with 1 h stop at every testing temperature. 5% N_2 was added and mixed to helium as a reference for chromatography. Gaseous and liquid components were analyzed by GC.

Hydrocarbon transformations were investigated with three different feedstocks: *n*-heptane (98.8%), hept-1-ene (97.3%), and liquid hydrocarbon mixture produced from CO and H_2 over FTS Co catalyst 20%Co/Al_2O_3. The experiments with hydrocarbon mixture were performed only with mixed Co–zeolite catalyst. The mixture contained (wt%): C_nH_{2n} (6.4–6.5), *n*-C_nH_{2n+2} (82.1–82.6), *iso*-C_nH_{2n+2} (11.0–11.5), C_5–C_{10} (51.9–53.7), C_{11}–C_{18} (36.7–37.3), C_{19+} (9.6–10.8).

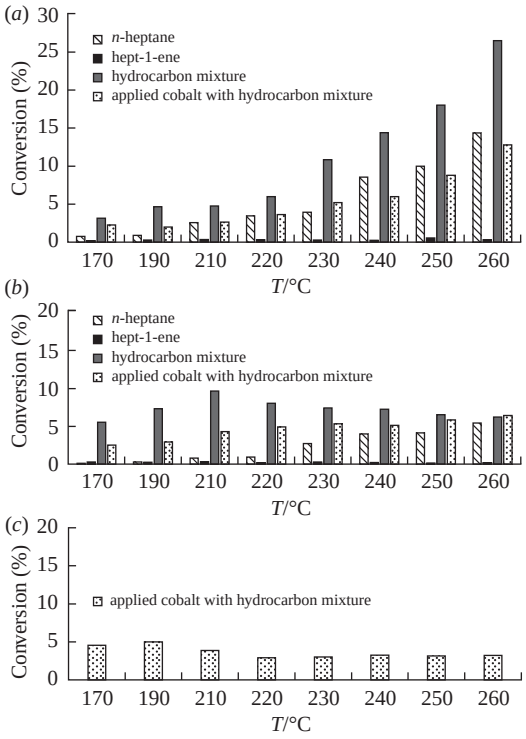

Figure 1 The temperature effect on the conversion of liquid hydrocarbons into gaseous products depending on the composition of the feed : *n*-heptane, hept-1-ene, hydrocarbon mixture, applied cobalt with hydrocarbon mixture and the type of catalyst system based on (*a*) HZSM-5, (*b*) HBeta and (*c*) zeolite-free (Ref).

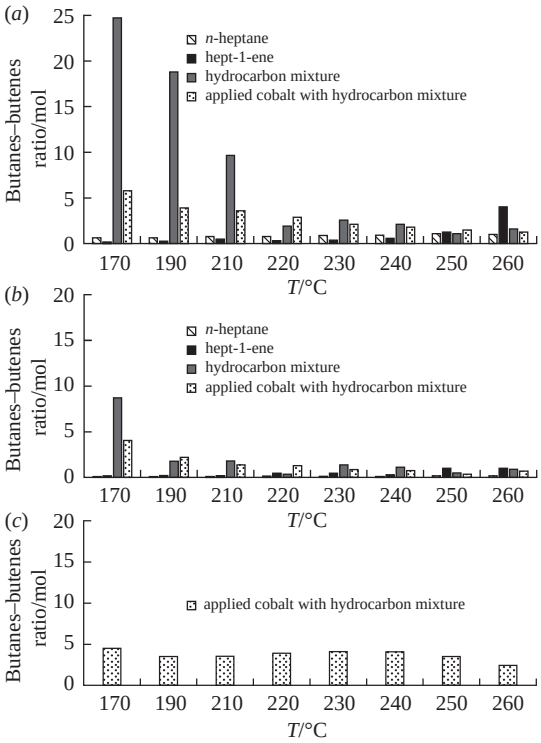

Figure 2 The temperature effect on the butane:butene ratio depending on the composition of the feed: *n*-heptane, hept-1-ene, hydrocarbon mixture and applied cobalt with hydrocarbon mixture and the type of catalyst system based on (*a*) HZSM-5, (*b*) HBeta and (*c*) zeolite-free (Ref).

20 mol%, respectively. Their formation in this oxygen-free process is explained by oxygen extraction from zeolite crystal lattice, which was confirmed by X-ray diffraction (Figure S2) and IR spectroscopy (Figure S3) studies of the zeolites before and after catalytic runs with hept-1-ene. Thus, CO and CO_2 were formed due to side interaction of adsorbed alkene molecules with zeolite crystal lattice (*cf.* ref. 12).

The conversion of hept-1-ene into other liquid hydrocarbons rose with temperature growth reaching 9% (Figure 3). The main product was *n*-heptane accompanied with isoheptanes up to 1 wt%. The formation of hydrogen-enriched paraffins inevitably should cause simultaneous production of carbon-enriched deposit on the surface of zeolites. Indeed, thermal analysis showed that the zeolites after run contained up to 20 wt% of heavy carbonaceous deposit (Figure S4).

The formation of heavy carbonaceous deposit on the zeolite surface correlates with the observed C_3/C_4 ratio in the gaseous product as well as with domination of alkenes in gas phase, *i.e.*, the deposit is also the cracking product [see Figure S1(*b*)]. This observation complies with reported data on alkene transformations over zeolites which starts with adsorption followed by polymerization/oligomerization and subsequent cracking.[13]

The *n*-heptane behavior was different from that of hept-1-ene. The conversion of *n*-heptane into gaseous products rose with temperature growth up to 8 and 5% over HZSM-5 and HBeta, respectively (see Figure 1). In the gas phase, C_4 hydrocarbons dominate, with butane:butene ratio rising with temperature. The C_3/C_4 ratio did not change significantly on temperature or zeolite variations stalling at the level of ~0.5. We believe that the observed C_3/C_4 hydrocarbons are formed by cracking of oligomers. It is remarkable that neither C_1–C_2 hydrocarbons nor carbon oxides were detected in the gas phase as distinct from the case of hept-1-ene. No significant conversion of *n*-heptane into other liquid hydrocarbons was observed. The carbonaceous deposit was still formed but in much lower amounts (Figure S4).

The results of transformation of hydrocarbon mixture cannot be explained as superposition effect of single alkane and alkene transformations observed in this work for model *n*-heptane and hept-1-ene. Some trends remind the dependencies for *n*-heptane such as conversion into gaseous products, which rose with temperature growth and was higher with HZSM-5 reaching 27% at 260 °C as compared to 12% in case of HBeta (see Figure 1). The gas phase contained mostly C_4 hydrocarbons, although the butane:butene ratio increased vastly as compared with individual heptane or heptene and reached 25 : 1. This ratio decreased rapidly to 1–2 with temperature raising to 260 °C (see Figure 2). The C_3/C_4 ratio in gas phase grew with temperature from 0.01–0.02 up to 0.2–0.3. The C_1–C_2 hydrocarbons and carbon oxides were not formed in hydrocarbon mixture transformation over HBeta (see Figure S1). However, in the course of transformation over HZSM-5 little ethylene was formed (0.5 mol%).

The changes in hydrocarbon liquid mixture composition depended on both reaction temperature and zeolite type (Figures 3 and 4). In the case of HZSM-5, the increase in C_{19+} fraction at 210–220 °C was observed as opposed by 5-fold drop at 250–260 °C [see Figure 4(*a*)]. The observed decrease in C_{19+} fraction at 170–190 °C can probably be dismissed as a result of adsorption of these heavy hydrocarbons at the surface (the control runs with inert contacts showed similar effect at 170–190 °C). The alkene conversion decreased slowly from 50 down to 25% through the whole temperature range [see Figure 3(*a*)]. A more complicated pattern was observed with C_5–C_{10} fraction, which can be explained by cracking activity of HZSM-5 growing significantly with temperature.

The HBeta-catalyzed transformation of liquid hydrocarbon mixture reached maximum at 240 °C [see Figure 3(*b*)]. The content of C_5–C_{10} fraction decreased at lower temperatures of 170–210 °C and rose at higher temperatures (Figure S5). The fact of alkene transformation [see Figure 3(*b*)] suggests that HBeta is less active than HZSM-5 in the investigated temperature range. It is interesting to note that both the zeolites are quite active in

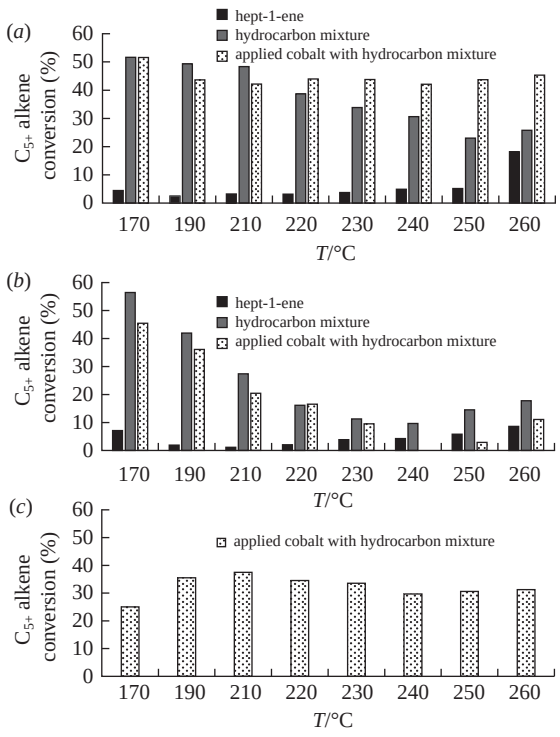

Figure 3 The temperature effect on the C_{5+} alkenes conversion depending on the composition of the feed: hept-1-ene, hydrocarbon mixture, applied cobalt with hydrocarbon mixture and the type of catalyst system based on (*a*) HZSM-5, (*b*) HBeta and (*c*) zeolite-free (Ref).

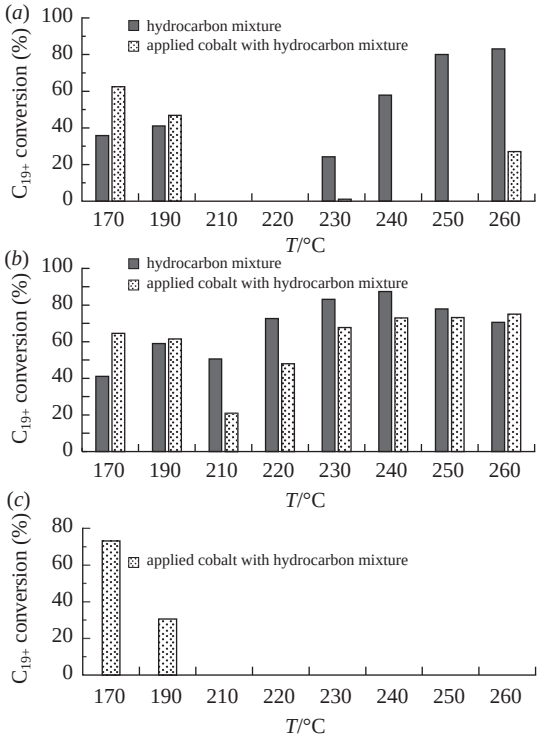

Figure 4 The temperature effect on the C_{19+} hydrocarbon conversion depending on the composition of the feed: hydrocarbon mixture, applied cobalt with hydrocarbon mixture and the type of catalyst system based on (*a*) HZSM-5, (*b*) HBeta and (*c*) zeolite-free (Ref).

isomerization of *n*-paraffins, with HBeta activity being significantly higher (Figure S5). Comparison of HSZM-5 and HBeta activities in respect of the increase in C_{11}–C_{18} fraction content suggests a lot of peculiarities in the transformation mechanism. Indeed, the HBeta-catalyzed transformation gives a ~7 wt% increase in C_{11}–C_{18} in all the temperature range, while HZSM-5-catalyzed process shows a maximum (11 wt%) increase at 170 °C and steep decline in this value down to 3 wt% at 260 °C. Apparently, HZSM-5 catalyzes mostly cracking of hydrocarbons while HBeta is active also in light alkene isomerization, alkylation and secondary cracking of heavy oligomerizates.

The interesting feature in the behavior of extruded Co catalysts was that these catalysts provided as twice as less gaseous products as compared with zeolites, which can be explained by partial blocking of zeolite active centers with deposited Co. With the Ref catalyst, conversion into gaseous products was even lower [see Figure 1(*c*)]. All the other dependencies found for zeolites were in line with those for the corresponding catalysts. In particular, the conversion into gaseous products decreased in sequence Co–HZSM-5 > Co–HBeta > Ref. Another feature is that the zeolite-catalyzed cracking leads to increase in the yield of propylene and C_3/C_4 ratio growth.

In the presence of all the catalysts, the formation of C_1–C_2, CO and CO_2 was negligible, showing slight increase in their yields with temperature, with a single exception being for zeolite-free catalyst.

The reaction temperature and the type of zeolite in a Co catalyst determined the changes in the composition of the liquid hydrocarbon mixture as well. Thus, in the presence of Co–HZSM-5, the conversion of C_{19+} hydrocarbons decreased from 62% at 170 °C to 27% at 260 °C, but at 210–220 °C the C_{19+} hydrocarbons were formed additionally [see Figure 4(*a*)]. Probably, the adsorption of C_{19+} hydrocarbons on the newly activated contact surface explains their transformation below 200 °C. The conversion of the C_5–C_{10} fraction in the presence of Co–HZSM-5 increased from 3 to 23–24% with temperature raising from 170 to 220–250 °C, but decreased down to 13% at 260 °C, which is probably due to more intensive cracking of C_{19+} hydrocarbons at higher temperature (Figure S6). Conversion of alkenes C_{5+} was 40–50% [see Figure 3(*a*)].

In the presence of the Co–HBeta catalyst, the conversion of C_{19+} hydrocarbons increased from 65% at 170 °C to 75% at 260 °C, but went through a local minimum of 21% at 210 °C, which was probably caused by adsorption of these components on the newly activated contact surface [see Figure 4(*b*)]. The conversion of the C_5–C_{10} fraction in the presence of this catalyst never exceeded 10% (see Figure S5). Conversion of alkenes C_{5+} was much higher at the same time and decreased from 45% at 170 °C to 11% at 260 °C due to competitive process of alkene formation by cracking of high-molecular components [see Figure 3(*b*)]. That is, the activity of Co–HBeta catalyst in cracking in the investigated temperature range was higher than that of Co–HZSM-5. It means that the addition of Co to zeolites leads to opposite effects on their cracking functions, *i.e.* increase in case of HBeta and weakening in case of HZSM-5.

In the presence of a reference catalyst, the conversion of C_{19+} hydrocarbons at 170–190 °C was 30–73% [see Figure 4(*c*)], which is also explained by adsorption on the freshly activated surface. In contrast, C_{19+} hydrocarbons were additionally formed at 210–260 °C undergoing, however, some cracking at the temperature close to 260 °C. Thus, the zeolite-free reference catalyst also has some cracking activity. The conversion of the C_5–C_{10} fraction in the presence of the Ref catalyst increased from 2 to 22% with the increase in temperature from 170 to 220–240 °C and decreased down to 18% at 260 °C (see Figure S5), which also indicates the presence of the cracking contact ability. However, the conversion of alkenes C_{5+} at the same time was 30–38% and practically did not depend on the reaction temperature [see Figure 3(*c*)], which indicated that the cracking reaction route was different from bimolecular one in this case.

The introduction of Co revealed distinctions in isomerization activity, namely, the Co–HBeta was as active as pristine zeolite,

while the introduction of Co into HZSM-5 led to suppression of isomerization (see Figure S5). The biggest uptake in alkene content caused by isomerization was detected as 4 wt% at 230–260 °C for Co–HBeta and 2 wt% at 250–260 °C for Co–HZSM-5. The activity of the Ref catalyst in isomerization was low.

The combination of the processes discussed above resulted in remarkable changes in the content of practically important C_{11}–C_{18} fraction (see Figure S5). The Ref catalyst gave 10 wt% uptake in C_{11}–C_{18} hydrocarbons in all the temperature range. Co–HZSM-5 provided higher value up to 14 wt%, while Co–HBeta never manifested more than 10 wt%. Both zeolite-based catalysts reveal complex temperature dependencies in C_{11}–C_{18} content changes, which is explained by overlapping of alkylation, oligomerization, cracking of C_{19+}, and secondary cracking of oligomerizates. Our suggestion is that in case of HZSM-5 the C_{11}–C_{18} hydrocarbons are formed mostly due to alkene-involved reactions of alkylation and oligomerization, while the growth of an average molecular weight is limited by cracking. It is probable that in case of the Ref catalyst the mechanism is similar with Lewis acid centers at the surface of Co mixed oxides responsible for this catalysis as well as for the formation of additional C_{19+}. The Co–HBeta was rather active in secondary cracking and isomerization, which resulted in lower average molecular weight.

Summarizing the experimental results reported, we can conclude that hydrocarbon transformations are catalyzed by both the HBeta and HZSM-5 zeolites at unusually low temperatures. The reaction route and product composition depend on both the zeolite type and feedstock. The distinction between different zeolites is most obvious in case of liquid hydrocarbon mixture but not individual hydrocarbons. The alkene transformation route includes the formation of heavy carbonaceous deposit on the zeolite surface due to oligomerization/condensation. The introduction of Co influences this process significantly. Finally, the conversion and distribution of liquid and gaseous products in the case of hydrocarbon mixture cannot be interpreted by simple superposition of individual hydrocarbon reactions and shows a kind of remarkable synergistic effect.

The results of this research shed a new light on the performance of multifunctional catalysts in the Fischer–Tropsch synthesis.

This study was supported by the Ministry of Science and Higher Education of the Russian Federation in terms of State Assignment to FSBI TISNCM.

Online Supplementary Materials

Supplementary data associated with this article can be found in the online version at doi: 10.1016/j.mencom.2020.03.023.

References

1 *Fischer–Tropsch Technology*, eds. A. Steynberg and M. Dry, Elsevier, Amsterdam, 2004, vol. 152.
2 W. Vermeiren and J.-P. Gilson, *Top. Catal.*, 2009, **52**, 1131.
3 C. Zhu and G. M. Bollas, *Appl. Catal., B*, 2018, **235**, 92.
4 C. Kibby, K. Jothimurugesan, T. Das, H. S. Lacheen, T. Rea and R. J. Saxton, *Catal. Today*, 2013, **215**, 131.
5 B. Sun, M. Qiao, K. Fan, J. Ulrich and F. Tao, *ChemCatChem*, 2011, **3**, 542.
6 T. Hanaoka, T. Miyazawa, K. Shimura and S. Hirata, *Chem. Eng. J.*, 2015, **263**, 178.
7 L. V. Sineva, E. Yu. Khatkova, E. V. Kriventseva and V. Z. Mordkovich, *Mendeleev Commun.*, 2014, **24**, 316.
8 L. V. Sineva, E. V. Kulchakovskaya, E. Yu. Asalieva and V. Z. Mordkovich, *Mendeleev Commun.*, 2017, **27**, 75.
9 G. Busca, *Heterogeneous Catalytic Materials*, Elsevier, Amsterdam, 2014.
10 *Zeolites and Catalysis*, eds. J. Cejka, A. Corma and S. Zones, Wiley–VCH, Weinheim, 2010.
11 L. V. Sineva, E. Yu. Asalieva and V. Z. Mordkovich, *Russ. Chem. Rev.*, 2015, **84**, 1176.
12 F. Eder, M. Stockenhuber and J. A. Lercher, *J. Phys. Chem. B*, 1997, **101**, 5414.
13 W. E. Farneth and R. J. Gorte, *Chem. Rev.*, 1995, **95**, 615.

Received: 15th August 2019; Com. 19/6012